International Journal of Modern Physics C

Forces by and on a Polymer Grafted to a Repulsive Wall

Jens Odenheimer
Institut für Theoretische Physik, Universität Heidelberg, Philosophenweg 19, D-69120 Heidelberg, Germany
j.odenheimer@tphys.uni-heidelberg.de

Michael Brill
Institut für Theoretische Chemie, Universität Heidelberg, Im Neuenheimer Feld 229, D-69120 Heidelberg, Germany
Michael.Brill@tc.pci.uni-heidelberg.de

Dieter W. Heermann
Institut für Theoretische Physik, Universität Heidelberg, Philosophenweg 19, D-69120 Heidelberg, Germany
heermann@tphys.uni-heidelberg.de

Received Day Month Year
Revised Day Month Year

We investigate a self-avoiding polymer chain anchored with one end at a hard wall. The chains are modeled using the continuous backbone mass model. The sampling of the conformations is done by molecular dynamics for chains of various sizes. Presented are results for several different interesting situations. We have investigated the pressure that grafted chains of various sizes exert on the wall and find good agreement with the theory, if the theory is extended to the self-avoiding case using the standard scaling laws. Force-elongation simulations are compared to polymer theory and the partition function for a grafted ideal chain is explicitly calculated. Again we find good agreement with the theory.

Keywords: grafted polymers; computer simulation; molecular dynamics; force-elongation behavior, pressure

PACS Nos.: 82.35.Gh, 82.35.Lr

1. Introduction

The properties of polymers grafted to a surface have been investigated extensively because of both scientific and technological importance in various processes. Polymers can be grafted or brought close to a hard wall as well as to a number of soft interfaces. These include surfactant or phospholipid bilayers in cells, in vesicles and in other membrane solutions [1]. Very interesting is the case of biological grafting. There, phospholipid bilayers build the walls of liposomes and cells, hosting proteins responsible for functions as diverse as anchoring the cytoskeleton [2]. When a polymer

is grafted to a bilayer it can induce gelation [3] or other phase changes [4,5] in liquid lamellar phases. They can also stabilize monodisperse vesicles [6]. Chemical modifications of both polymeric and ceramic membranes by polymer grafting and graft polymerization techniques have demonstrated improved fouling resistance of microfiltration and ultrafiltration membranes [7] and improved selectivity and stability of pervaporation membranes [8]. Ultrathin end-grafted polymer layers also play an important role in colloidal stabilization [9,10], chromatography, adhesion [11], lubrication, microelectronics and biocompatibility of artificial organs in medicine [12].

When a polymer chain is brought in the neighborhood of a repulsive, impenetrable wall, the number of conformations available to the chain is reduced [13,14]. The average configuration of the polymer is a compromise between the need to avoid the wall and the constraint imposed by the grafted end of the chain. Thus the statistics of conformations will be influenced and it is therefore of theoretical interest to analyze the consequences of the grafting and of the restriction to a half space. Attempts to analyze the situation have been made analytically as well as by various numerical methods.

Theoretical studies of polymers near surfaces deal mostly with adsorbing walls. On such systems surface phase transitions occur. A thorough review of these transitions is provided by De'Bell and Lookman [15]. They studied adsorption of general SAW's, stars and other topologies on planar surfaces, wedges and slabs. A detailed field theoretical review is written by Diehl [16] and high order ϵ-expansion studies have been done by Zinn-Justin et al [17]. Semi-infinite systems undergoing phase transitions are treated, e.g. by Lipowsky [18]. Monte Carlo studies were made by Rabin et al. [19]. Lai and Binder [20,21,22] used the bond fluctuation model of polymer chains on lattices to do Monte Carlo simulations. They studied layers of polymers anchored with one end at a hard wall, assuming good solvent conditions and repulsive interactions between the monomers and the wall. Also molecular dynamics simulations of polymer brushes have been done by Murat and Grest [23]. They looked at various quantities with respect to the surface coverage. Hegger and Grassberger [24] performed Monte Carlo simulations of polymers near an adsorbing surface.

The majority of the above-mentioned works deal with polymers near an adsorbing wall and for grafted polymers, mainly brushes were treated. The theory of polymers in constrained geometry mostly deals with Gaussian chains due to the complexity of the constraint. The simulations are mainly Monte Carlo under good solvent conditions with bulk density. We have done molecular dynamics simulations on a single grafted polymer with excluded volume interaction grafted to a repulsive wall and thus we do not expect the theoretical work mentioned above to fully hold. Since our wall is athermal we observe no surface phase transition and the studies (theoretical or numerical) cannot be fully used for comparison. The aim of this work is thus to see whether the existing theories apply to our case. Throughout this paper we shall refer to the ungrafted self-avoiding chain as *free* as opposed to the grafted chain.

In chapters 3 and 4 of the paper we investigate the pressure field induced by the polymer onto the wall. Due to the reduction of conformational entropy a non-homogeneous pressure field is created acting on the wall in a region comparable to the polymer size. The results are compared to the theory developed by Bickel et al. [25,26]. Interactions between membranes and polymers are also studied in detail by Lipowsky [27]. A polymerized membrane in confined geometry and the conformation of fluid membranes are treated by Gompper and Kroll [28,29]. In chapters 5 and 6 the force-elongation behavior of a polymer grafted to a wall is investigated. The simulational results are compared to the existing polymer theory where three force regimes are distinguished. Further the partition function for an ideal chain grafted to a wall is calculated and the resulting force-elongation behavior is compared with the simulation.

2. The Polymer Model

In this work the continuous backbone mass model [30] is used. It allows to study the entropic effects on the wall as well as further studies using realistically modeled biopolymers. The model interpolates between the united atom model and the bead-spring model. In contrast to these two models it uses non-spherical force fields for the non-bonded interaction. The main idea of this approach with a more general form of the force field is to generalize the united atom model in a way that larger atom groups are combined to one construction unit, but the possible anisotropy of these groups is still taken into account. The simplest anisotropic geometrical object one can think of is an ellipsoid of rotational symmetric form and thus it is considered as the interaction volume of the chemical sequences in our model. As one wants the force field to degenerate into a sphere with increasing distance, we use a con-focal force field inside this interaction volume:

$$\mathcal{H}_{\text{inter}} = V_{\text{abs}} \left(\frac{d_1^{(p)} + d_2^{(p)}}{2} - c \right), \tag{1}$$

where $d_1^{(p)}$ and $d_2^{(p)}$ denote the distance of the point $\mathbf{p}$ to the focal points of the ellipsoid and V_{abs} is the absolute potential. For convenience we use only a repulsive part

$$V_{\text{abs}}(r) \sim r^{-6} \qquad . \tag{2}$$

The mass of the building units is distributed between the focal points of the ellipsoids in the hard core region of the con-focal potential. The main ingredient of the model is the mass matrix of our rod-chains. In order to construct it, we must first calculate the Lagrangian of a single rod $\mathcal{L}_i = T_i - V_i$ with the kinetic energy T_i and the potential energy V_i. The subindex i marks the position of the rods in the chain. This one-dimensional homogeneous rod i has the length l_i starting at $\vec{a}_i$ and ending at $\vec{b}_i$. If we suppose that the rods all have the same mass m and that the velocity

of the rod mass scales linearly with the position between the boundaries of the rod, the kinetic energy can be written as

$$\begin{aligned} T_i &= \frac{1}{2}\int_0^{l_i} \frac{m}{l_i}\left(\frac{(l_i-x)\dot{\vec{a}}_i + x\dot{\vec{b}}_i}{l_i}\right)^2 dx \\ &= \frac{1}{6}m(\dot{\vec{a}}_i{}^2 + \dot{\vec{a}}_i\dot{\vec{b}}_i + \dot{\vec{b}}_i{}^2). \end{aligned}$$

Adding the single terms of the rods building the chain we get the Lagrangian $\mathcal{L}$ of the whole rod chain. The equations of motion of the chain can be calculated from the Lagrange equations of the second kind. Since the equations of motion separate in each direction, we have only to solve three tridiagonal $(N+1)\times(N+1)$ matrices per chain which consist of N rods per time step of the form

$$\mathbf{W}\ddot{\vec{x}} = \vec{F} \tag{3}$$

$$\frac{m}{6}\begin{pmatrix} 2\,1\,0\,0\ldots \\ 1\,4\,1\,0\ldots \\ 0\,1\,4\,1\ldots \\ \vdots\,\vdots\,\vdots\,\vdots\,\ddots \end{pmatrix}\begin{pmatrix} \ddot{x}_0 \\ \ddot{x}_1 \\ \ddot{x}_2 \\ \vdots \end{pmatrix} = \begin{pmatrix} F_{10} \\ F_{11}+F_{21} \\ F_{22}+F_{32} \\ \vdots \end{pmatrix} \tag{4}$$

with the force F_{ij} on the coordinate j of the flexible point i of the chain

$$F_{ij} = -\frac{\partial V_i}{\partial j} \tag{5}$$

and $\ddot{x}_i$ denote the accelerations of the flexible points of the chain. The flexible points are the link points of the ellipsoids and the end points of the rod chain. The sub-indices mark the positions in the chain: 0 and $N+1$ are the end-points of the chain and the numbers between them denote the linking points of rods in the chain. The bonded interactions between neighboring units are given by harmonic length and angle potentials:

$$\mathcal{H}_{bond} = \frac{1}{2}k(r-r_0)^2 \tag{6}$$

$$\mathcal{H}_{angle} = \frac{1}{2}k_\theta(\cos\theta - \cos\theta_0)^2 \tag{7}$$

with the bond lengths r and the bending angles θ. Here r_0 and θ_0 denote the mean values.

3. Mean-Field Theory for the Pressure that a Grafted Chain exerts on the Wall

Consider a wall with a repulsive r^6 potential and a polymer grafted at the wall. The constraint that the polymer is grafted and that one half-space is excluded leads to a competition between the necessity to avoid the wall and the constraint to be fixed at the wall. Due to the entropy the monomers would like to stay as far away from the wall as possible. In order to do so they exert a pressure on the wall [25,26]. This

pressure decreases radially from the grafting point. For a theoretical treatment of the pressure we shall regard an elastic wall. Following [26], let the surface of the wall be described by $h(x, y)$. The thermodynamic properties of the chain of length N grafted at the repulsive wall can be described by the propagator $G_N(\vec{r}, \vec{r}')$ resulting from the Edwards equation

$$\frac{\partial G_N(\vec{r}, \vec{r}')}{\partial N} = \frac{l^2}{6} \Delta G_N(\vec{r}, \vec{r}') \tag{8}$$

with the $G_N(\vec{r}, \vec{r}') = 0$ at the wall and $\lim_{N\to 0} G_N(\vec{r}, \vec{r}')$
$= \delta(\vec{r}, \vec{r}')$. The partition function is then given by

$$Z_N(l) = \int d\vec{r}' G_N(\vec{r}, \vec{r}') \quad , \tag{9}$$

where the integral extends over all space that is available to the free end. The Greens-function for a planar wall $h(x, y) = 0$ can then be factorized as

$$G_N^{(0)}(\vec{r}, \vec{r}') = \left(\frac{3}{2\pi N l^2}\right)^{3/2} \exp\left[-\frac{3(x-x')^2}{2Nl^2}\right] \exp\left[-\frac{3(y-y')^2}{2Nl^2}\right] \times \left(\exp\left[-\frac{3(z-z')^2}{2Nl^2}\right] \exp\left[-\frac{3(z+z')^2}{2Nl^2}\right]\right) \quad .$$

The partition function is therefore

$$Z_N^{(0)}(l) = \int_{-\infty}^{+\infty} dx' \int_{-\infty}^{+\infty} dy' \int_0^{+\infty} dz' G_N^{(0)}(\vec{l}, \vec{r}') \tag{10}$$

$$= \mathrm{erf}\left(\frac{l}{2R_g}\right) \quad , \tag{11}$$

where $R_g = \sqrt{Nl^2/6}$ is the radius of gyration of the free chain and erf the error function. To compute the pressure we introduce a small perturbation in h. We can write the partition function as $Z_N = Z_N^{(0)} + Z_N^{(1)} + Z_N^{(2)} + \ldots$, where $Z_N^{(i)}$ is of order h^i and Z_N^0 as in (10). Due to the linearity of (8), each term satisfies the Edwards equation

$$\frac{\partial Z_N^{(i)}}{\partial N} = \frac{l^2}{6} \Delta Z_N^{(i)} \quad i = 0, 1, 2, \ldots \tag{12}$$

The solutions of higher orders are coupled to the constraint. Now we have

$$\begin{aligned} 0 &= Z_N(x, y, h) \\ &= Z_N(x, y, 0) + h(x, y) \frac{\partial Z_N}{\partial z}(x, y, 0) + \frac{h^2(x, y)}{2} \frac{\partial^2 Z_N}{\partial z^2}(x, y, 0) + \ldots \quad . \end{aligned}$$

For the linear contribution $Z_N^{(1)}$ we get

$$Z_N^{(1)}(x, y, 0) = -h(x, y) \frac{\partial Z_N^{(0)}}{\partial z}(x, y, 0) \quad , \tag{13}$$

yielding [26]

$$Z_N^{(1)}(\vec{l}) = \frac{l^2}{6}\int_0^N dn \int dS \frac{\partial G_{N-n}^0}{\partial z}(x,y,0;\vec{a}) Z_n^{(1)}(x,y,0) \quad . \tag{14}$$

Hence, the change in the height is, to first order, due to the work

$$\begin{aligned} \Delta W &= W[h] - W[0] \\ &= -k_B T \log\left[1 + \frac{Z_N^1}{Z_N^0}\right] \\ &= \int dS p(x,y) h(x,y) \quad , \end{aligned}$$

where $p(x,y)$ has the symmetric form

$$p(r) = \frac{k_B T}{2\pi (r^2+l^2)^{3/2}} \left(1 + \frac{r^2+l^2}{2R_g^2}\right) \exp\left[-\frac{r^2+l^2}{4R_g}\right] \tag{15}$$

with $r = \sqrt{x^2+y^2}$. To push at $\vec{r} = (x,y)$ an elementary volume of $dV(r) = h(r)dS$ we need the work $dW = p(r)h(r)dS$. The function $p(r)$ is the pressure. The entire entropic force which the chain exerts on the wall is then given by

$$F = \int_0^\infty dr 2\pi r p(r) = \frac{k_B T}{l} \exp\left[-\frac{l^2}{4R_g^2}\right] \tag{16}$$

$$= \frac{k_B T}{l} \exp\left[-\frac{3}{2N}\right] \quad . \tag{17}$$

4. Simulation Results

We have simulated 10 different chain lengths $N = 20, N = 40, N = 60, N = 80, N = 100, N = 125, N = 150, N = 175, N = 200$ and $N = 250$ to study the pressure and the corresponding finite effects. In Figure 1 the finite-size scaled radius-height distribution is shown. The height and radius are divided by their respective radii of gyration. In Figure 2 we show the finite-size scaling plot for the pressure distribution. The full curve is the fit using the predicted form of the distribution (see (15)). The fit is very good over the entire region. We do not sample data too close to the grafting point because the statistics are too strongly biased by the finite excluded volume interaction of the monomers with the first grafted monomer. Note that the theory was developed for Gaussian chains and hence the coefficients of the fit cannot be expected to be identical to theory. Nevertheless, we see that the functional form of the finite-size scaling distribution fits well to the prediction. In Figure 3 is shown the entropic force exerted on the wall by the polymer. The figure gives the result for the Gaussian and for the chain with self-avoidance. We can see that for increasingly larger chains the difference between Gaussian and self-avoiding chains becomes negligible and the extrapolated lines coincide at zero to the value of one within errors. Notably the self-avoiding chain always applies a greater entropic pressure on the wall than the Gaussian chain. This difference is greatest for small

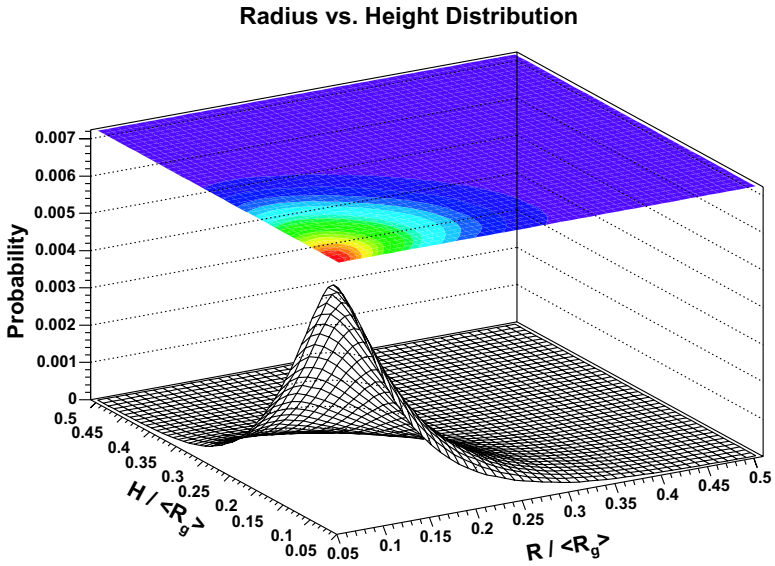

Figure 1. Shown is the distribution of the height with respect to the radius. The values are divided by their respective radii of gyration for reasons of finite-size scaling.

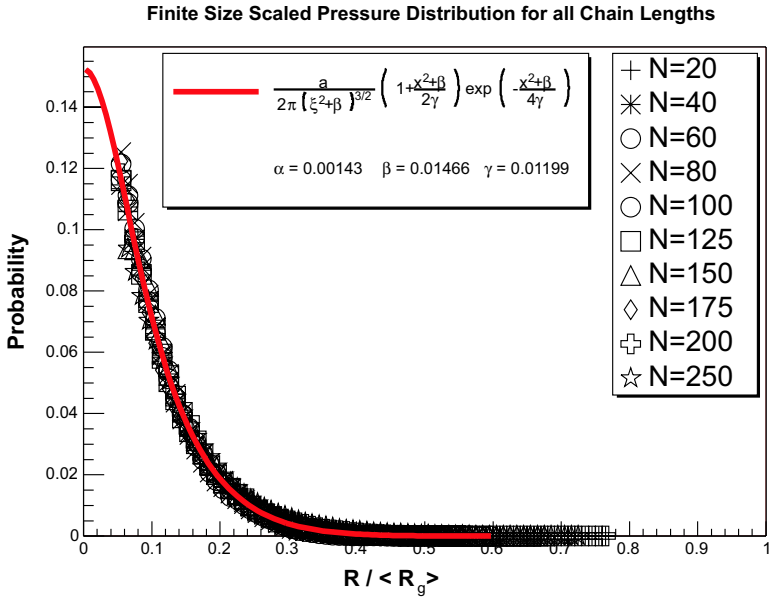

Figure 2. Finite-size scaling plot for the pressure distribution. The full curve is the fit using the predicted form of the distribution. The fit is very good over the entire region.

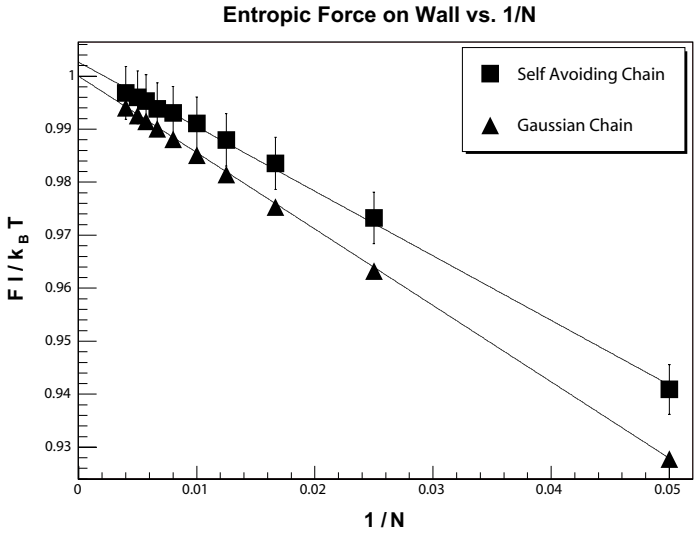

Figure 3. Shown is the entropic force exerted on the wall by the polymer. The figure gives the result for the Gaussian and for the chain with self-avoidance.

chains and diminishes in the infinite chain limit. This means that for short chains we observe that excluded volume effects contribute a significant part to the total force. The fact that the chain needs to avoid itself and is grafted at the same time creates an additional force. For long chains entropy clearly dominates the force due to the geometric restriction to a half space and the contribution from self-avoidance becomes negligible. This does not mean that generally self-avoidance can be neglected for long chains. Indeed we have shown quite the opposite for various quantities, especially for the ratio of the end-to-end radius and the radius of gyration. For the entropic component of the force on the wall however, we do observe that the geometric restriction outweighs the self-avoidance. Note that Figure 3 shows only the entropic component and not the force due to the monomer-wall force-field interaction, which is substance-specific and hence not of interest for an arbitrary chain.

5. Force-elongation behavior

Following the arguments of [13], [31] and [32] it is possible to derive the following results. Knowing the distribution function, we can calculate the partition function of the polymer with an external force:

$$Z = \int d\vec{r} p_N(\vec{r}) \exp\left(\frac{\vec{f}\cdot\vec{r}}{T}\right). \tag{18}$$

But it is also possible to derive the desired results by fundamental reasoning. We only need to introduce the two characteristic lengths for the problem, $R_F \cong lN^{\nu}$

and $\xi_p = T/f$. In general, the norm of the mean end-to-end distance vector can be written as:

$$\left|\left\langle \vec{r}(\vec{f})\right\rangle\right| = R_F \varphi_r \left(\frac{R_F}{\xi_p}\right) = R_F \varphi_r(x), \tag{19}$$

where $\varphi_r(x)$ is a dimensionless function. In the case of small forces one expects a linear response of the polymer, so that we can write $\lim_{x\to 0} \varphi_r(x) \cong x$. Using this we get:

$$\left|\left\langle \vec{r}(\vec{f})\right\rangle\right| \cong \frac{R_F^2}{T} f. \tag{20}$$

If the chain is stretched stronger, we expect deviations from the linear law. Let us assume that the stretched chain is composed of "blobs", i.e. small chain-balls. Each of these blobs has a size of ξ_p. In such a blob the external force is just a small perturbation, so we can write for the number of monomers g_p in the blob:

$$\xi_p \cong l g_p^{\nu} \tag{21}$$

or:

$$g_p = \left(\frac{T}{lf}\right)^{1/\nu}. \tag{22}$$

Considering that the number of the blobs must be N/g_p, one obtains for the three-dimensional case:

$$\left|\left\langle \vec{r}(\vec{f})\right\rangle\right| \cong \frac{N}{g_p}\xi_p \cong Nl\left(\frac{fl}{T}\right)^{0.689}. \tag{23}$$

Hence for large forces the elongation behavior is not linear. For the case of stretched polymers one can look again at the distribution function, which has the form $\exp(-(r/R_F)^{\delta})$. The resulting entropy is:

$$S(r) = \text{const} + \ln \mathrm{p_N(r)} = \text{const} - \left(\frac{\mathrm{r}}{\mathrm{R_F}}\right)^{\delta}. \tag{24}$$

In this case the corresponding elastic free energy amounts to:

$$F_{tot} = T\left(\frac{r}{R_F}\right)^{\delta} - fr. \tag{25}$$

If one minimizes this expression, one obtains the wanted relation between force and end-to-end distance:

$$f \cong \delta \frac{T}{R_F}\left(\frac{r}{R_F}\right)^{\delta-1}. \tag{26}$$

We have seen how to calculate the relation between applied force and resulting elongation for long chains with self-avoiding as well as without self-avoiding. In the next section we will compare the expected analytical behaviour with simulation results.

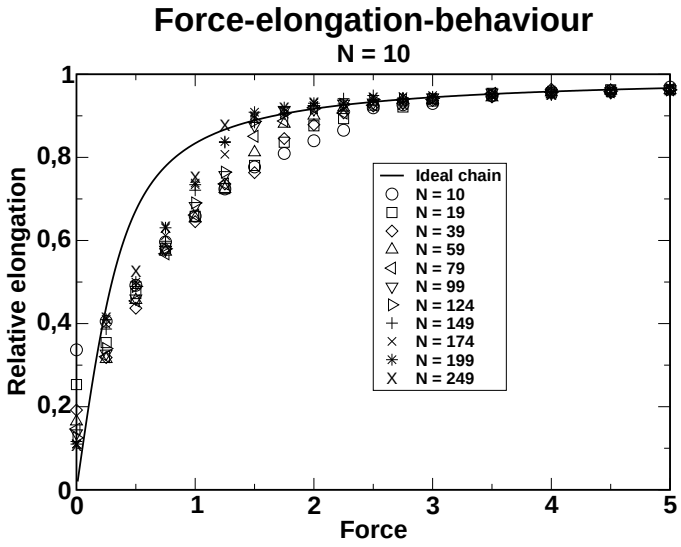

Figure 4. Shown are the force-elongation simulation results for all simulated chain lengths compared to the ideal chain behavior.

6. Simulation Results

In figure (4) all simulation results are shown compared with the ideal chain behavior. One can see significant deviations in the low and medium force range. Especially, these parts will be compared to the existing theory.

First we will take a look at the simple case of large forces. This case is characterized by a highly stretched chain. In this state the monomers cannot interact with the wall or other monomers in the chain. This causes a behavior that is close to that of a highly-stretched ideal chain where no wall is used and where the monomers have no interaction potentials. In figure (5) this large force region is shown for some chains. This behavior can be found for any chain length.

If one compares a typical simulation result of the stretch simulation with the ideal chain behavior, one can see that there is a deviation for small and medium forces. This deviation is caused by the wall and the self-avoiding property of the polymer. For the medium force range we have a force-elongation prediction as shown in the previous section, see equation (23). Now we try to identify this $f^{0.689}$-behavior. Therefore we fit a power-law to the simulational data in the 0.5 to 1.5 force units range. We receive an exponent for every data set that is about 0.55 as shown in figure (6). This is not a really good match. The difference between the obtained exponent and the theoretical may be caused by the wall or the finite size of the polymers. But because of the wall one would expect a higher not a smaller exponent. The polymer tries to arrange away from the wall, so it should be easier

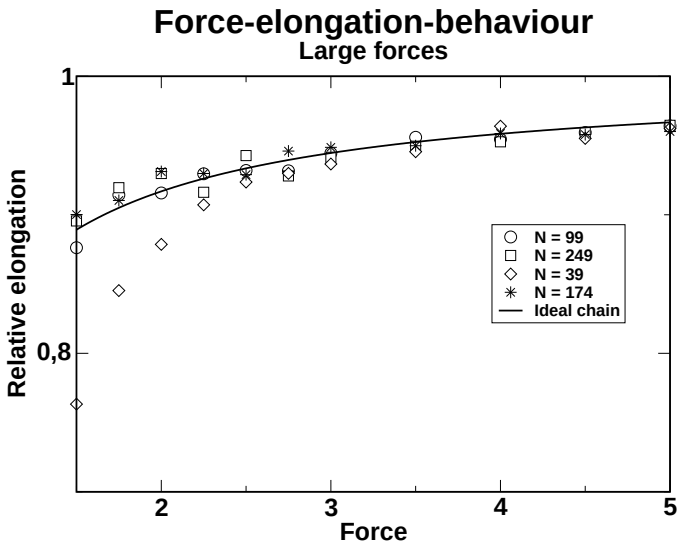

Figure 5. End-to-end-distance for large forces

to stretch the chain which should lead to a higher exponent. The interesting thing about this is the fact that the exponent is hardly changing in the analyzed length interval. Another point for the mismatch could be the accuracy of the method how the $f^{0.689}$-law was derived.

In the small-force range we have two predictions for the force-elongation behavior, one for simple random walks and the other for the self-avoiding walks. In both cases a linear behavior is predicted. In the ideal case we expect a fix spring constant for any polymer length, but in the self-avoiding case the spring constant depends of the chain length. Now we will investigate if this dependence is reproduced by the simulations. But first the theoretical spring constants

$$k_{id} = \frac{l}{3T} \tag{27}$$

$$k_{sa} = \frac{lN^{0.184}}{T} \tag{28}$$

(here "id" means ideal and "sa" means self-avoiding). The fit to the data is shown in figure (7), where we can see the spring constant for different polymer lengths. We see that there is a dependence of the chain length, so we can disregard the ideal chain result. Now we have to fit a power-law to the spring constant data to obtain the exponent. The result for the fit is 0.26 ± 0.01 which is too high compared with the predicted $N^{0.184}$-law.

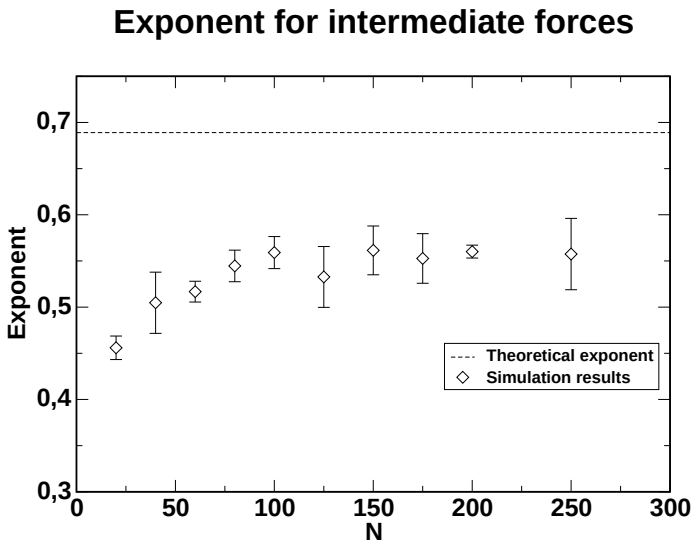

Figure 6. Elongation exponent for intermediate forces

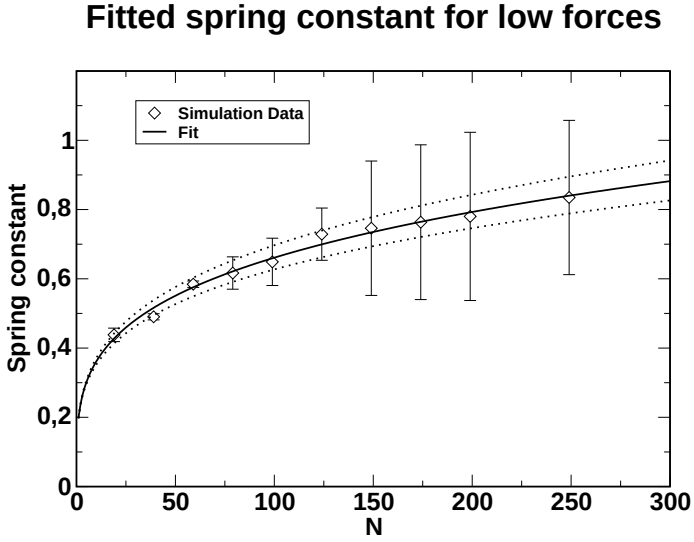

Figure 7. Spring constants for the low force range

6.1. *Comparison of short chains with the ideal chain fixed at a wall*

In figure (8) the results for the 10-monomer chain are shown representative for the short chains. Here, one can see the typical differences that also occur for the

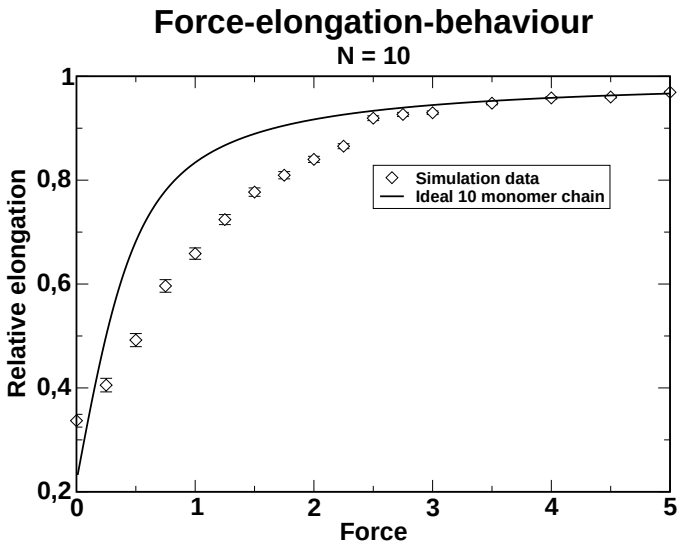

Figure 8. Force-elongation behavior for 10 monomer chains

longer chains. At the low and medium force range one can see the effects of the self-avoiding-property. Here, in both cases the wall is included, in the simulation as well as in the ideal chain calculation. Because of the high complexity of the calculations they were only made up to the 10-monomer chain.

7. Discussion

We have presented in this paper simulation results for polymer chains grafted to an impenetrable wall. Two main questions were addressed. First, we looked at the pressure. As suggested the polymer exerts pressure on the wall to which it is grafted. The pressure exerted by the polymer chain is very high close to the grafting point and decays sharply over a distance of order R_g. Our data fit very well the predictions from Bickel et al. who granted that the values of the coefficients differ due to the self-avoidance. Finally, we did see that the difference between the self-avoiding chain and the Gaussian chain diminishes at large N. Second, we looked at the force-elongation behavior of the polymer chain. The comparison to the polymer theory has shown that the wall influences the predicted power laws that were derived for the unconstrained polymers. Further the contribution of the wall and the self-avoiding property of the polymer force-elongation behavior were pointed out. At intermediate forces the deviation from the ideal chain behavior is dominated by the self-avoiding property and at low forces mainly the wall is responsible for the offset in the force-elongation curves.

8. Acknowledgment

We would like to thank E. Eisenriegler, K. Binder and P. Grassberger for helpful discussions.

Bibliography

1. S. Safran, *Statistical Thermodynamics of Surfaces, Interfaces and Membranes*, Addison-Wesley, Reading, MA (1994)
2. B. Alberts, D. Bray, A. Johnson, J. Lewis, M. Raff, K. Roberts, P. Walter, *Molecular Biology of the Cell*, Garland Publishing, New York (1998)
3. H.E.Warriner, S.H.J. Idziak, N.L. Slack, P. Davidson, C.R. Safinya, *Science* **271**, 969 (1996)
4. Y. Yang, R. Prudhomme, K.M. McGrath, P. Richetti, C.M. Marques, *Phys. Rev. Lett.* **80**, 2729 (1998)
5. G. Bouglet, C. Ligoure, A.-M. Bellocq, E. Dufourc, G. Mosser, *Phys. Rev. E* **57**, 834 (1998)
6. R. Joannic, L. Auvray, D.D. Lasic, *Phys. Rev. Lett.* **78**, 3402 (1997)
7. R.P. Castro, H.G. Monbouquette, Y. Cohen, *J. Membr. Sci.* **84**, 151 (1993)
8. D.-J. Jou, W. Yoshida, Y. Cohen, *J. Membr. Sci.* **162**, 269 (1999)
9. D. Napper, *Polymeric Stabilization of colloidal Dispersions, Academic Press London*, (1983)
10. A. Gast and L. Leibler, *Macromolecules* **19**, 686 (1986)
11. L. H. Lee, *Adhesion and Adsorption of Polymers*, Plenum Press New York, (1980)
12. E. Ruckenstein and D.B. Chang, *J. Colloid Interf. Sci.* **123**, 170 (1988)
13. P.-G. De Gennes, *Scaling Concepts in Polymers Physics*, Cornell University Press, Ithaca (1979)
14. E. Eisenriegler, *Polymers Near Surfaces*, World Scientific, Singapore (1993).
15. K. De'Bell and T. Lookman , *Rev. Mod. Phys.* **65**, 87 (1993)
16. H. W. Diehl, *Phase Transitions and Critical Phenomena* **10** (1986)
17. J.C. Le Guillou and J. Zinn-Justin, *Phys. Rev. Lett.* **46**, L137 (1985)
18. R. Lipowsky, *Phys. Rev. Lett.* **49**, 1575 (1982)
19. E. Duering and Y. Rabin, *Macromolecules* **23**, 2232 (1990)
20. Pik-Yin Lai and Kurt Binder, *J. Chem. Phys.* **95**, 9288 (1991)
21. Pik-Yin Lai and Kurt Binder, *J. Chem. Phys.* **97**, 586 (1992)
22. Pik-Yin Lai and Kurt Binder, *J. Chem. Phys.* **98**, 2366 (1993)
23. M. Murat and G. S. Grest, *Macromolecules* **22**, 4054 (1989)
24. R. Hegger and P. Grassberger, *J. Phys. A* **27**, 4069-4081 (1994)
25. T. Bickel, C. Marques, C. Jeppsen, *C. R. Acad. Sci. Paris, t. 1, Series IV*, 661, (2000)
26. T.Bickel, C.M. Marques and C. Jeppesen *Euro. Phys. J. E* (2001)
27. R. Lipowsky, *Physica Scripta.* **T29**, 259-264 (1989)
28. G. Gompper and D. M. Kroll, *Europhys. Lett.* **15**, 783 (1991)
29. G. Gompper and D. M. Kroll, *Science* **255**, 968 (1992)
30. G. Schöppe and D.W. Heermann, *Phys. Rev. E.* **59**, 636 (1999)
31. Alexander Yu. Grosberg and Alexei R. Khokhlov. *Statistical Physics of Macromolecules* AIP Press, (1994)
32. D.W. Heermann K. Binder. *Monte Carlo Simulation in Statistical Physics*. Springer, Heidelberg (2002)